







Review

Recent Advances in Ultrasound Breast Imaging: From Industry to Clinical Practice

Orlando Catalano ¹, Roberta Fusco ^{2,*}, Federica De Muzio ³, Igino Simonetti ⁴, Pierpaolo Palumbo ^{5,6} , Federico Bruno ^{5,6} , Alessandra Borgheresi ^{7,8}, Andrea Agostini ^{7,8}, Michela Gabelloni ⁹ , Carlo Varelli ¹, Antonio Barile ¹⁰ , Andrea Giovagnoni ^{7,8}, Nicoletta Gandolfo ¹¹, Vittorio Miele ^{6,12}  and Vincenza Granata ⁴ 

¹ Department of Radiology, Istituto Diagnostico Varelli, 80126 Naples, Italy

² Medical Oncology Division, Igea SpA, 80013 Naples, Italy

³ Department of Medicine and Health Sciences “V. Tiberio”, University of Molise, 86100 Campobasso, Italy

⁴ Division of Radiology, “Istituto Nazionale Tumori IRCCS Fondazione Pascale-IRCCS di Napoli”, 80131 Naples, Italy

⁵ Department of Diagnostic Imaging, Area of Cardiovascular and Interventional Imaging, Abruzzo Health Unit 1, 67100 L’Aquila, Italy

⁶ Italian Society of Medical and Interventional Radiology (SIRM), SIRM Foundation, 20122 Milan, Italy

⁷ Department of Clinical, Special and Dental Sciences, University Politecnica delle Marche, 60126 Ancona, Italy

⁸ Department of Radiology, University Hospital “Azienda Ospedaliera Universitaria delle Marche”, 60126 Ancona, Italy

⁹ Department of Translational Research, Diagnostic and Interventional Radiology, University of Pisa, 56126 Pisa, Italy

¹⁰ Department of Applied Clinical Sciences and Biotechnology, University of L’Aquila, 67100 L’Aquila, Italy

¹¹ Diagnostic Imaging Department, Villa Scassi Hospital-ASL 3, Corso Scassi 1, 16149 Genoa, Italy

¹² Department of Emergency Radiology, Careggi University Hospital, 50134 Florence, Italy

* Correspondence: r.fusco@igeamedical.com

Abstract: Breast ultrasound (US) has undergone dramatic technological improvement through recent decades, moving from a low spatial resolution, grayscale-limited technique to a highly performing, multiparametric modality. In this review, we first focus on the spectrum of technical tools that have become commercially available, including new microvasculature imaging modalities, high-frequency transducers, extended field-of-view scanning, elastography, contrast-enhanced US, MicroPure, 3D US, automated US, S-Detect, nomograms, images fusion, and virtual navigation. In the subsequent section, we discuss the broadened current application of US in breast clinical scenarios, distinguishing among primary US, complementary US, and second-look US. Finally, we mention the still ongoing limitations and the challenging aspects of breast US.

Keywords: ultrasound; breast imaging; clinical practice



Citation: Catalano, O.; Fusco, R.; De Muzio, F.; Simonetti, I.; Palumbo, P.; Bruno, F.; Borgheresi, A.; Agostini, A.; Gabelloni, M.; Varelli, C.; et al. Recent Advances in Ultrasound Breast Imaging: From Industry to Clinical Practice. *Diagnostics* **2023**, *13*, 980. <https://doi.org/10.3390/diagnostics13050980>

Academic Editor: Ernest Usang Ekpo

Received: 29 December 2022

Accepted: 2 March 2023

Published: 4 March 2023



Copyright: © 2023 by the authors. Licensee MDPI, Basel, Switzerland. This article is an open access article distributed under the terms and conditions of the Creative Commons Attribution (CC BY) license (<https://creativecommons.org/licenses/by/4.0/>).

1. Introduction—Where Do We Come from?

In 1977, Dr. Dodd wrote: “The spatial resolution presently obtainable in ultrasonograms is inadequate for the detection of subclinical [breast] cancer” [1]. Later still in 1983, Sickles and co-workers claimed: “These data indicate that sonography is not an acceptable substitute for mammography in the detection and diagnosis of breast cancer” [2]. For many years, the main use of breast ultrasound (US) was for differentiating cystic lesions from solid lesions [3]. Consequently, US has become an integral component of the diagnostic work-up of breast abnormalities only in the last two decades [4–8]. The seminal article on using US for differential diagnosis was only published in 1995 [9], and the first BI-RADS atlas addressing the issue of US, in addition to mammography, was only published in 2003 [10]. The dramatic increase in spatial resolution is the main explanation for the advancing role of US. The application of tissue harmonics, spatial compound imaging, and speckle reduction techniques further refined the images [3,11]. Appropriate scanner settings and optimized scanning methodologies are also mandatory for an up-to-date US examination of the breast.

Technological advances now allow a comprehensive US diagnosis, management, and treatment of breast abnormalities. In this review, we discuss the technical revolution that happened over the years and point out the consequent clinical revolution that has occurred in daily practice.

2. Technological Developments—What the Industry Has Made Available to Us

2.1. Conventional Doppler Techniques and New Microvasculature Imaging Techniques

Cancer growth is based on neoangiogenesis, i.e., the tumor-induced development of a vascular network. Detecting these flow signals and assessing their characteristics in terms of number, distribution, and appearance are consequently of paramount importance in tumor characterization and monitorization [12–28]. Even if appropriately set to identify small, low-flow vessels, conventional Doppler techniques, including color Doppler and power Doppler, have a limited sensitivity. In recent years, almost all companies have developed filtered techniques capable of working at a higher frame rate and consequently detecting tiny intra- and peri-tumoral flow signals. With these new software facilities, the background and tissue motion artefacts are suppressed and US sensitivity, spatial resolution, and temporal resolution are significantly improved [29–38]. Some companies have also developed systems capable of quantifying the number of colored pixels within the box, thus quantifying the flow intensity [39]. If a new microvascular tool is available on the scanner, we encourage users to refrain from still using conventional Doppler modalities for breast imaging and to employ more advanced techniques (Figure 1).

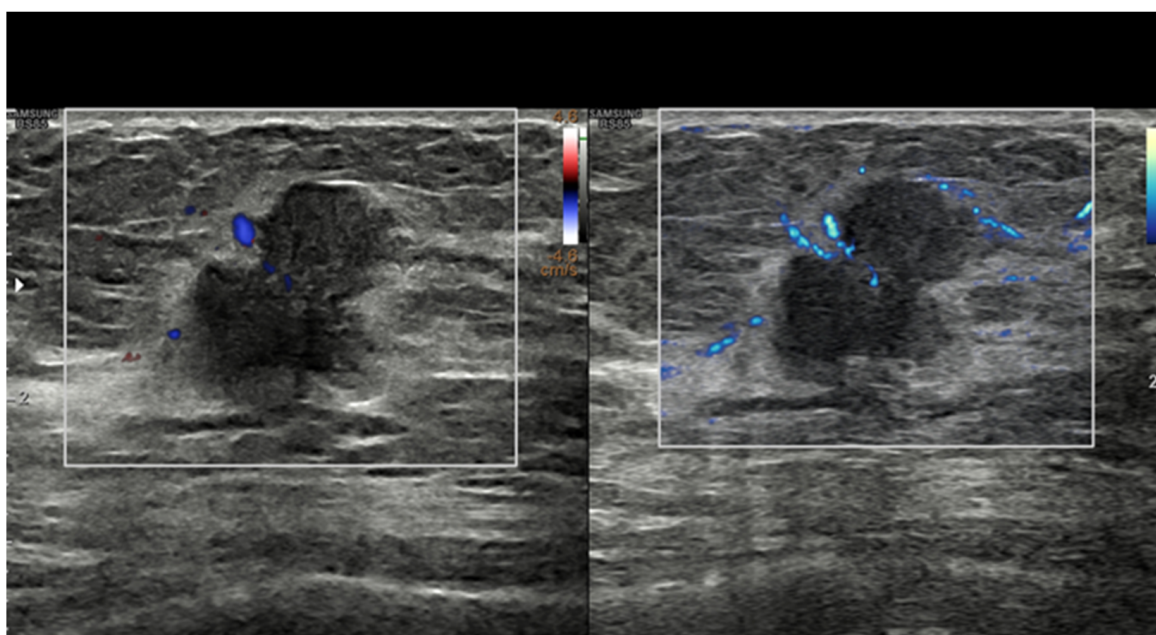


Figure 1. Breast invasive ductal carcinoma. Vascularization as assessed with power Doppler (**left**) and with MV-Flow (**right**). Recently developed techniques such as MV-Flow are more sensitive to slow flows and offer a better display of tumor vessels.

2.2. High-Frequency Transducers

The transmission frequencies employed to scan breasts have increased through the years, moving from 7.5 MHz initially to 10–12 MHz and currently to 13–18 MHz. High-frequency transducers provide increased axial and soft tissue resolution, permitting improved differentiation of subtle shades of gray, margin resolution, and lesion conspicuity in the background of normal breast parenchyma [11]. Current transducers have a broad band of frequencies, allowing the operator to choose the most appropriate one in relation to the size of the given breast and based on the depth of the area of interest within it. However, most US companies now sell probes reaching frequencies up to 22–24 MHz. These trans-

ducers have been developed to study the skin, but there are a number of circumstances where they can be adopted to investigate the breast. These include skin abnormalities of the breast and axilla, nipple–areolar complex abnormalities, very small-size breasts, superficial areas in any size breasts, prepuberal breasts, male breasts, breast parenchyma abnormalities in subjects with implants, post-mastectomy chest wall, and intraoperative breast sonography [32] (Figure 2).

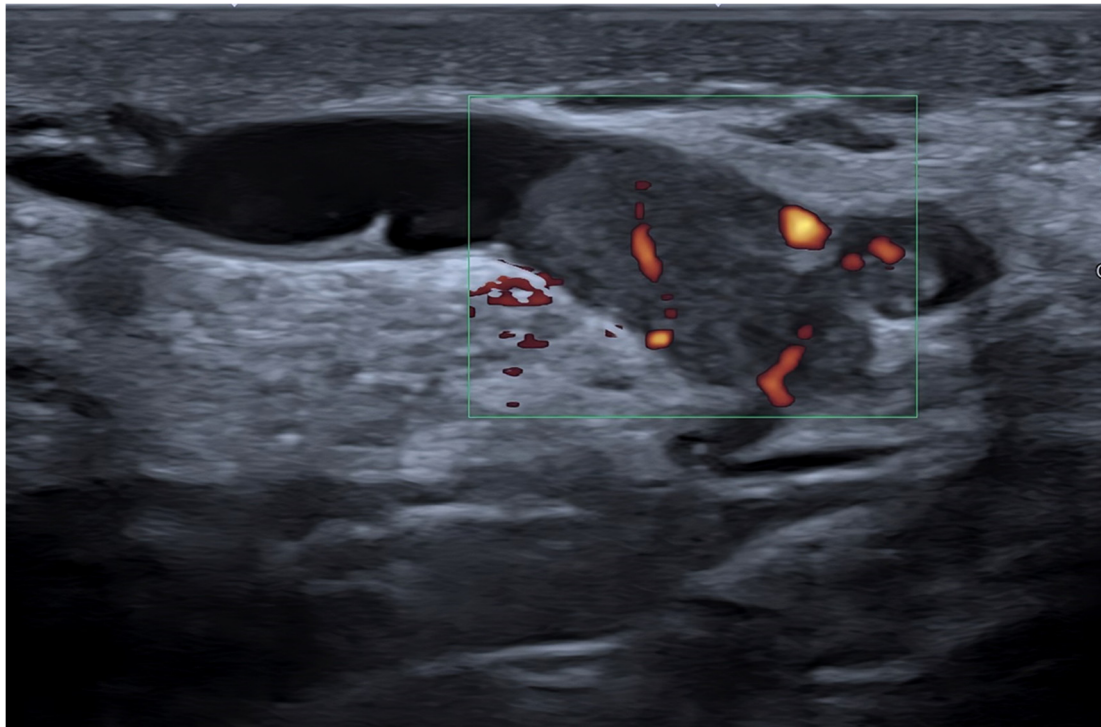


Figure 2. Breast intraductal papilloma. Detailed morpho-structural assessment working with a high-frequency transducer (22 MHz). Power Doppler detection of tumor vessels.

2.3. Extended Field-of-View Scanning

US has a limited field of view (FOV), not allowing to display, in a single scan, a breast area larger than the probe footprint itself [11]. Extended FOV systems allow to partially encompass this limitation. Starting from a real-time translational movement of the probe over the skin, the software can continuously compare the position and create a large 2D image, without any loss in terms of spatial resolution.

Extended FOV scans allow to display and measure large breast lesions. Additionally, it becomes possible to show the spatial relationship and the distance between a lesion and some anatomic landmarks, such as the nipple, or between multiple lesions, as for multifocal/multicentric cancer [13] (Figure 3). Images of the whole implant can be obtained, being particularly useful for plastic surgeons.

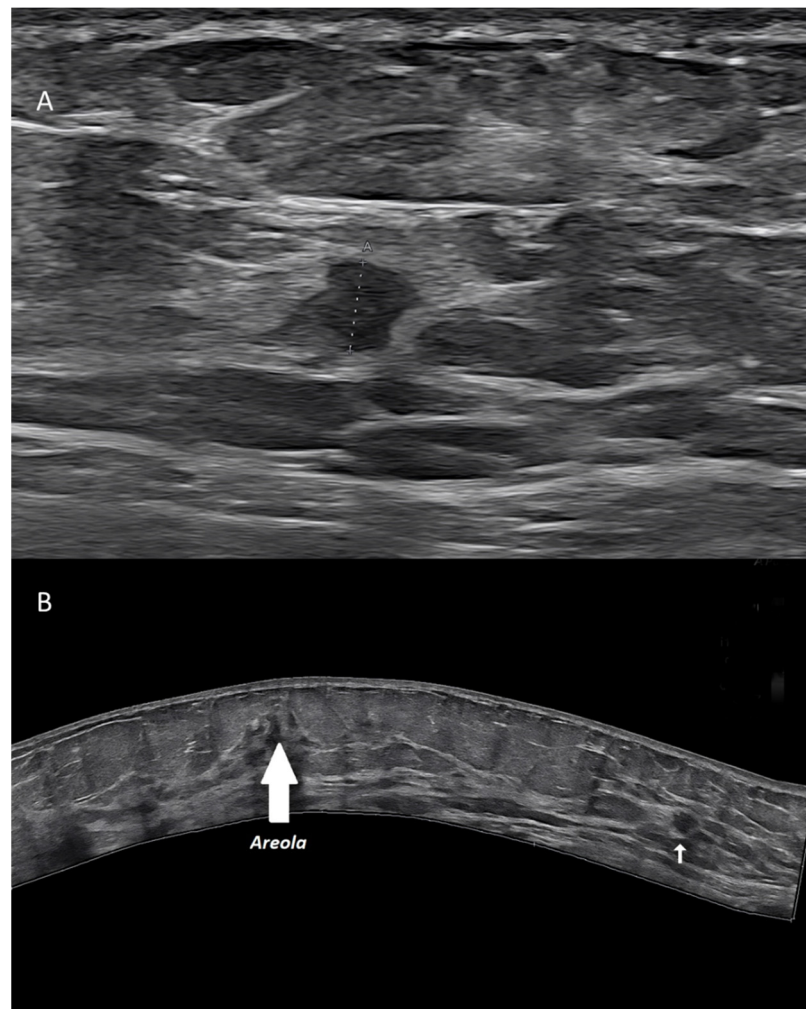


Figure 3. Invasive ductal carcinoma of the breast. (A) US scan showing a 4-mm nodule (calipers). (B) Extended FOV scan displaying the nodule (arrow) within the whole breast.

2.4. Elastography

US elastography measures small tissue motions due to pressure forces, i.e., the viscoelastic properties of breast abnormalities [40]. Current techniques include strain elastography, based on the manual pressure from the operator; acoustic radiation force impulse imaging (ARFI); point shear-wave elastography; and 2D/3D shear-wave elastography, based on the changes provoked from the focused ultrasounds themselves. Based on the different techniques, qualitative (subjective scoring), semi-quantitative (strain-to-fat ratio), and/or quantitative data can be obtained [7,8,37,41–49].

The use of elastography has been mostly focused on breast nodule characterization, but aspects such as tumor detection, tumor extent assessment, axillary lymph node status, percutaneous procedure guidance, and tumor response to treatment assessment must also be considered [41,50–52]. As a general rule, stiffer nodules (i.e., score 1 or 2, low strain ratio, low shear-wave speed), opposing a significant resistance to the changes, are thought to be malignant, while elastic ones (i.e., score 4 or 5, high strain ratio, high shear-wave speed) are usually categorized as benign [53] (Figure 4).

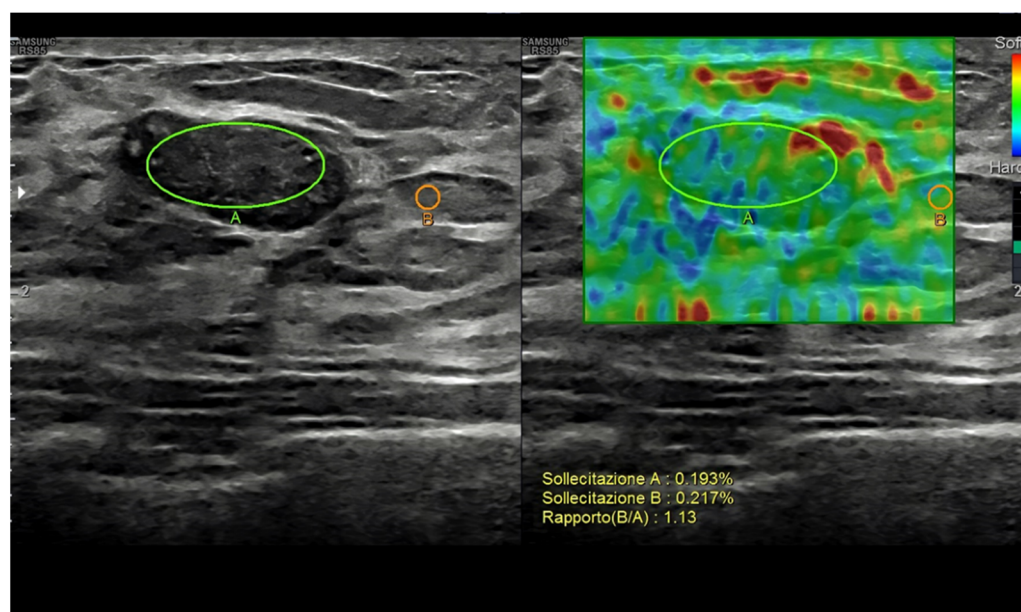


Figure 4. Breast fibroadenoma. Strain ratio allows a semi-quantitative assessment of the lesion-to-fat stiffness.

Breast nodules may, however, show an intermediate behavior (score 3), with overlapping findings and possible false positives (fibrotic and calcified fibroadenomas, sclerosing adenosis, radial scar, steatonecrosis, etc.) and false negatives (e.g., lymphomas, in situ ductal carcinomas, and small or low-grade or tubular invasive carcinomas) [54,55]. Elastography may increase US specificity, although this may come at the cost of decreased sensitivity. Consequently, images' interpretation should never rely on elastography alone and should always be correlated with the grayscale appearance [53,56].

2.5. Contrast-Enhanced Ultrasound

As for Doppler vascular signal, the intensity of contrast medium enhancement represents an indirect indicator of tumor microvascular density, correlating with a malignant nature and with the cancer grade. First introduced to boost the low-sensitivity Doppler systems of the 1990s, microbubble contrast media are now employed during real-time, low mechanical-index, grayscale US. However, despite a high number of publications, contrast-enhanced US (CEUS) has not significantly impacted breast imaging. This is mostly due to the kind of contrast media available until now, which work better at the low frequencies employed to scan the abdomen than at the higher frequencies needed to image superficial structures such as the breast [57–62].

Malignant breast nodules show a quick and strong but transient enhancement, with variable degrees of heterogeneity [63–67]. Irregular, tortuous, radially distributed vessels are seen around and inside tumors [35]. A time–intensity curve can be obtained to quantify the microbubbles' behavior over time. Three-dimensional images may better render the tumor angioarchitecture [68]. CEUS may measure the tumor size better than conventional B-mode US. Additionally, it may assess the breast tumor response to neoadjuvant treatment, showing 87% aggregated sensitivity and 84% aggregated specificity in a recent meta-analysis [69]. Tissue harmonic imaging (THI) and contrast harmonic imaging (CHI) also have value in the detection and characterization of breast tumors.

2.6. Three-Dimensional Ultrasound

Both hand-held and automated linear transducers are available for use in high-resolution 3D breast imaging. Three-dimensional US, also called volumetric US, allows for obtaining a surface rendering of normal and abnormal breast structures. With a single pass of the ultrasound beam, a 3D reconstructed image is formed in the coronal, sagittal,

and transverse planes, allowing a more accurate assessment of anatomical structures and tumor margins [11]. Coronal images, being parallel to the skin, represent a unique opportunity allowed from 3D US. A vivid representation of breast tumors can be obtained, with a retraction, star-like profile strongly supporting the diagnosis of malignancy [70–74] (Figure 5).

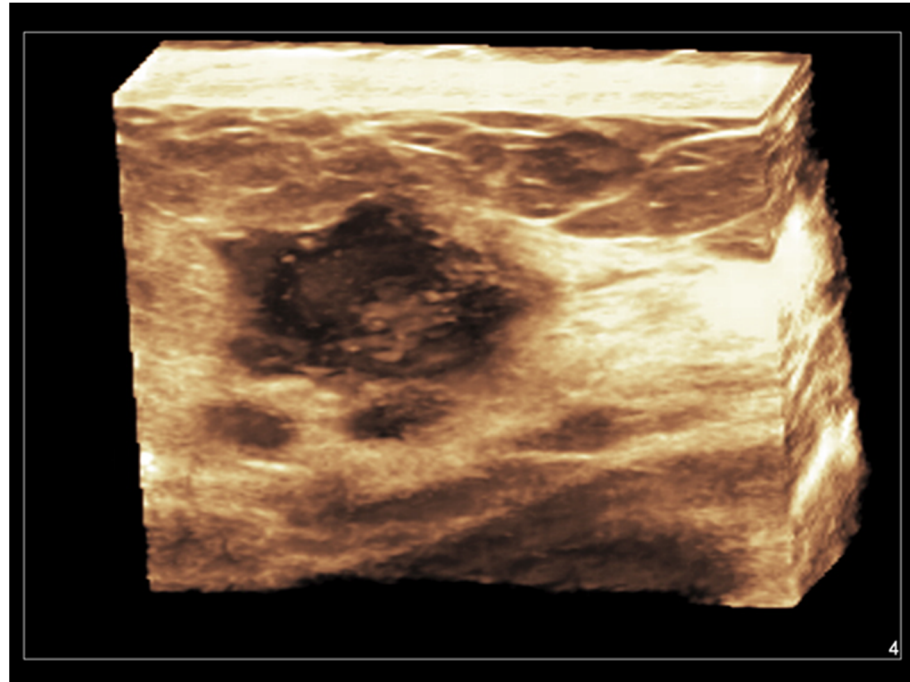


Figure 5. Invasive ductal carcinoma of the breast. Coronal 3D display of infiltrating tumor margins.

Additionally, lesions can be automatically or semi-automatically delimited on the three planes, and their volumes can be quantified. Nodules' growth and cancer regression during treatment can be objectively evaluated through serial scans. Three-dimensional US can be combined with harmonic imaging, Doppler techniques, and CEUS [16]. Additionally, percutaneous procedures can be advantaged by viewing multiplanar and three-dimensional images.

2.7. *MicroPure*

Grouped microcalcifications represent a very important finding in breast imaging and a significant US limitation, being hard or impossible to detect, particularly if not associated with a nodule [75]. *MicroPure*TM is a software from Canon (Tokyo, Japan) that allows to highlight microcalcifications (Figure 6).

MicroPure combines non-linear imaging with speckle suppression, extracting the calcification from the heterogeneous background. Filtered microcalcifications are shown as bright dots inside a dark blue background overimposed to a grayscale US.

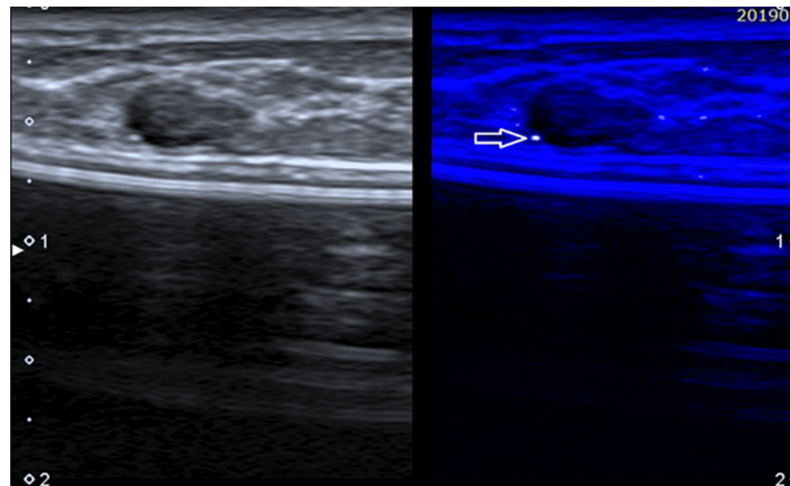


Figure 6. Fibroadenoma in a patient with history of augmentation mammoplasty. MicroPure allows to easily detect a bright dot (arrow) due to a small calcification.

2.8. Automated Breast Ultrasound

So-called “manual” or “hand-held” US is limited by operator dependence, non-reproducibility, and the inability to image extensive breast areas and store volumes [64]. To overcome these limitations, an automated breast US (ABUS) system, or automated breast volume US, has been developed. ABUS allows a technologist to simultaneously acquire large volumes of tissue, from the skin to the chest wall, by using a large, specific transducer (15 cm) [76,77]. These volumes, consisting of a high number of thin scans, are stored to be visualized and reformatted by a doctor at another moment or another place. Coronal views are of special value [78]. By now, ABUS has been considered an adjunct to mammography to screen patients with dense breasts. ABUS has shown good agreement with manual US in terms of detection rate and BI-RADS categorization [79–81]. Architectural distortions and peritumoral infiltrations may be better displayed than with manual US, while large masses can be easily measured [82]. A good correlation with MRI in the assessment of tumor response to treatment has been demonstrated [81]. ABUS is less time-consuming than manual US and causes less fatigue to the operator [64]. It should be considered, however, that any probe-mediated palpation finding is missed with ABUS and that the direct interaction between the patient and the physician is completely lost.

2.9. Computer-Assisted Diagnosis—S-Detect

Owing to deep learning algorithms, artificial intelligence systems are able to automatically detect and quantify a number of features from US images [16,68,83–90]. This may allow for the simple and reproducible detection and characterization of breast lesions as well as the prediction of the response to treatment in patients with locally advanced breast cancer. Computer-assisted diagnosis (CAD) can be employed as a second reader to improve the accuracy of the operator in US or CEUS imaging of the breast [64,91–93]. The software analyzes the targets identified by the operator, showing their shape and their risk of malignancy based on the BI-RADS lexicon or other descriptors. A CAD system works through four successive phases: pre-processing, segmentation, feature extraction and selection, and classification [64,94]. The analysis can be approved or rejected by the operator [95,96].

CAD systems can be offline, located in a personal computer, or inserted directly on the scanner. An example of the latter is represented by S-DetectTM, a semi-automatic tool from Samsung (Busan, Republic of Korea) [97–100]. The operator manually places a marker inside a lesion, and then, the software traces the border (adjustable) and analyzes and classifies the lesion according to the US descriptors from the BI-RADS (Figure 7).

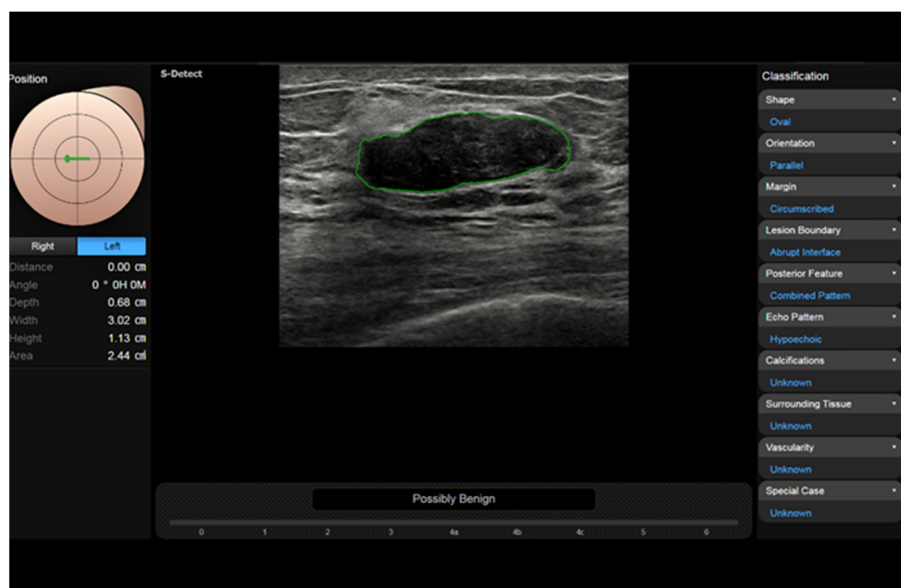


Figure 7. S-Detect automatic measurement and categorization of a breast nodule (fibroadenoma) using BI-RADS descriptors.

In a study on the differential diagnosis of breast lesions, the sensitivity of five operators of different experience levels was >90% and specificity was 50–75%, while S-Detect had 90% sensitivity and 71% specificity [101]. Advanced systems are fully automatic, are based on convolutional neural networks, and have a high capability of recognizing the images.

2.10. Ultrasound Nomograms

Radiomics can extract many quantitative features from US images through a computer algorithm [102]. To create a nomogram, first, well-established US features are selected and extracted by the training experts; then a model is built; and finally, the model is tested, possibly using both an internal and an external validation cohort of patients. The quantitative features extracted through computerized algorithms can be employed for the differential diagnosis of breast abnormalities or to predict the prognosis (risk of lymph-node metastasis, risk of high nodal burden, etc.) or establish in advance the response to treatment of breast tumors [103].

2.11. Images Fusion and Virtual Navigation

Fusion imaging consists of merging digital images from two different modalities to improve the overall performance, with special reference to lesions' localization at second-look US and to the percutaneous approach to those abnormalities poorly visible with US. Real-time images of the US system are combined (directly overimpressed or shown synchronized side by side) with those previously uploaded from a previous mammography, CT, MRI, or PET exam. This allows real-time, virtual navigation through the volume. The structures invisible under US but visible with other modalities can be operated using US-guided biopsy navigated by the other modality [64]. The indirect systems employ artificial skin markers placed before the exam, while the direct systems use some anatomical landmarks as spatial references [104–106]. Algorithms have been developed for assessing organ motion induced by breathing and movement [64].

BreastNav[®] is an interesting system from Esaote (Genoa, Italy) allowing fusion between a prone MR scan and a supine US scan through 2D remodeling applied to the breast from an anatomical landmark established during the MR scans. An electromagnetic sensor is applied to the transducer. This allows a targeted second-look US assessment of findings not determined at MRI. The US fusion volume navigation technique can be used to scan the breast nodules requiring follow-up [64].

Needle-tracking software facilities, based on specific sensors, allow to simulate the needle path during US-guided percutaneous procedures. This tool may increase effectiveness and safety.

3. Changing Clinical Scenarios—The Current Impact of US in Breast Practice

3.1. Primary Ultrasound

There are a good number of clinical settings where whole-breast, bilateral, axilla-including US must be regarded as the first imaging modality to be employed, after physical examination. In many circumstances, US will be conclusive to solve the issue, while in others, US results will prompt further investigation.

A palpable breast mass or swelling always requires imaging assessment, and US will effectively differentiate cysts (BI-RADS 2), non-suspected nodules (BI-RADS 3), and suspected nodules (BI-RADS 4 and 5) [11,14,107–109].

Dense breasts in young women cannot be imaged efficaciously with mammography. However, more and more women nowadays are asking for an imaging assessment to feel themselves followed and to reduce their anxiety. These subjects can be asymptomatic or may present with symptoms such as breast pain or tenderness. US has become the supplemental screening tool of choice for cancer detection in women with dense breast tissue.

MRI is the most effective tool in measuring the primary breast tumor extent, and it allows the detection of additional foci of mammographically and/or sonographically occult disease in women with newly diagnosed cancer. However, US is also useful for preoperative breast cancer staging, with special reference to axillary lymph nodes' status, allowing to perform examination of the whole axilla with level 1–3 lymph nodes.

Nipple discharge, a common circumstance of special relevance if bloody or dark, can now be imaged with US. Galactography is no longer employed, and MRI is reserved to selected cases.

US works well for newborns, children, and adolescents with breast abnormalities (grading of premature thelarche, etc.). Breast disorders in pregnancy should be studied using US, at least because of radioprotection needs [11]. Lactating breasts are also difficult to image with mammography because of the glandular density, and US is the primary imaging modality in women with abnormal symptoms during lactation [11]. Male breast abnormalities should be studied with US, which can easily differentiate gynecomastia from cancer. Breast assessment in women scheduled for augmentation surgery or for hormonal therapy because of infertility is also based on US, particularly for younger women. Periodic assessment after mastoplasty is carried out with US, while MRI is employed when an implant rupture is suspected [110] (Figure 8).



Figure 8. Sub-muscular breast implant as displayed using an extended FOV acquisition.

Owing mainly to the real-time characteristic, US is the method of choice to guide diagnostic and therapeutic percutaneous procedures whenever the target is adequately visible with US [111–114]. US can also be useful during treatment planning for breast radiation therapy [11]. Intraoperative US can guide the surgeon towards a quicker and more effective approach at the operating table, decreasing the incidence of positive margins and the consequent need for re-excision [11].

Though focused on the mammary parenchyma, breast US has the ability to assess all the tissue layers, from superficial to the gland (dermis and hypodermis) and deeper to the gland (retro-glandular fat, chest wall, and pleuro-pulmonary area) (Figure 9).

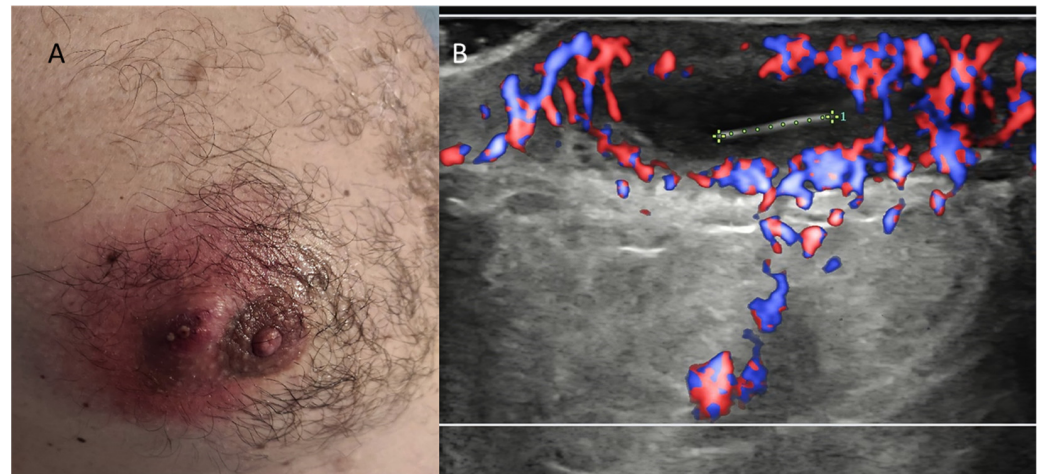


Figure 9. Ingrown areolar hair causing abscess formation in a young male. (A) Clinical photograph. (B) Power Doppler US imaging. The 6-mm linear echogenic hair and the surrounding strong hyperemia are readily recognizable, allowing a confident differential diagnosis with Montgomery glands inflammation.

Patients presenting to a US exam for abnormalities arising from these areas, as well as non-glandular incidental findings during breast US, can be readily evaluated. Second-level imaging modalities are employed in selected cases [14,33,107–118].

3.2. Complementary Ultrasound

US is both an adjunct and a complement to mammography (Figure 10).

Screening of asymptomatic women is based on mammography. However, younger women are now asking to be imaged for an early diagnosis of breast cancer. In this setting, mammography alone is not enough, and combination with US, or with ABUS, is mandatory [115–119].

Surveillance of women at high risk, bearing a hereditary/familial risk, is currently performed with contrast-enhanced MRI. However, US can represent a useful adjunct, at least to increase the time interval between each MRI exam. US complements initial mammography and, if needed, MRI in the assessment of local and regional tumor extent. MRI is the gold standard in the assessment of response to treatment both in patients with neoadjuvant therapy for a locally advanced breast cancer and in patients with a metastatic breast cancer. However, being an easily repeatable exam, US can be performed serially and allows multiple measurements of the size changes. US complements annual mammography in the loco-regional follow-up of patients with a history of breast cancer [120,121].

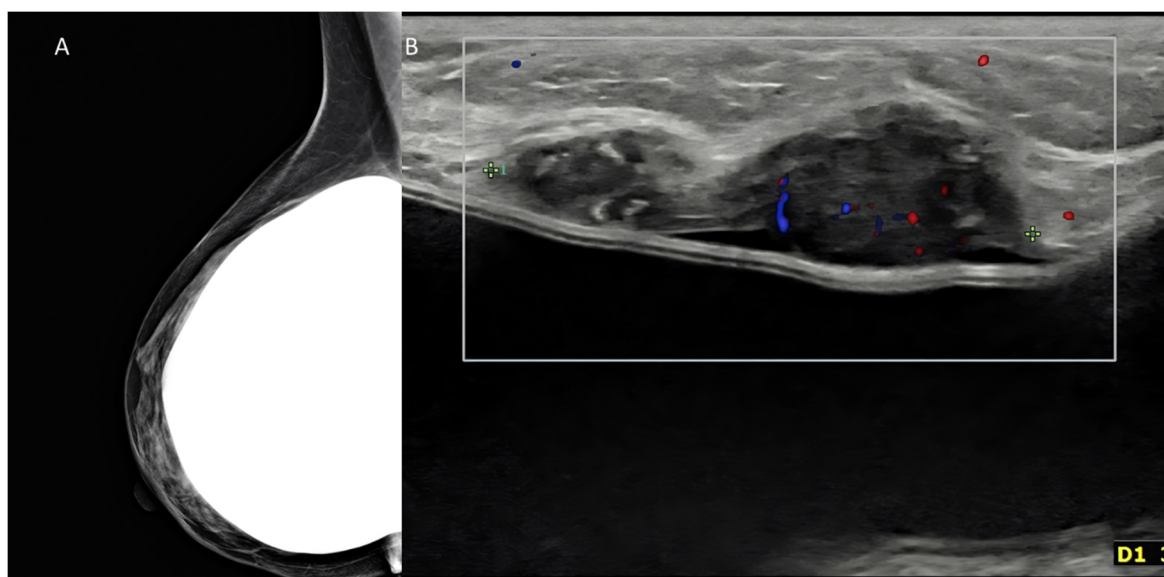


Figure 10. Palpable mass in a woman with history of augmentation mammoplasty. (A) Mammography oblique digital view was negative in this case, despite use of tomosynthesis. (B) US could detect a nodule immediately above the implant. The tumor proved to be a triple-negative invasive ductal carcinoma at surgery.

3.3. Second-Look Ultrasound

US is frequently used as a targeted, second-look option for patients imaged with other breast imaging modalities.

Since the beginning, US has been employed to better define any abnormality found with mammography. US is employed to differentiate cystic and solid opacities, to assess the level of suspicion of any nodule, and to assess distortion or any other changes. US is performed immediately after a mammography requiring further work-up or during patient recall. Finally, US is employed in patients with a palpable abnormality and negative mammograms.

Contrast-enhanced MRI may require a targeted US scan in the case of enhancing or apparently enhancing focal changes or when an intense background parenchymal enhancement may mimic or masquerade a breast nodule [82,122,123]. Lesions detected on MRI are often mammographically occult, but many of them can be detected with targeted US [11]. Lesions found with MRI can be located by US and, consequently, can be histologically clarified by US-guided biopsy [64].

Breast uptakes with a whole-body PET scan can also be further investigated with US to avoid false positive diagnoses. This applies to patients undergoing a PET exam because of breast cancer but also to subjects with non-mammary primary tumors during their staging or follow-up with molecular imaging.

Breast nodules are frequently detected during contrast-enhanced or unenhanced CT exams, chest scans, abdominal scans, or whole-body scans (Figure 11).

US works well as a quick and simple tool to confirm or rule out a nodule and to establish the need for further investigation or for patient follow-up.

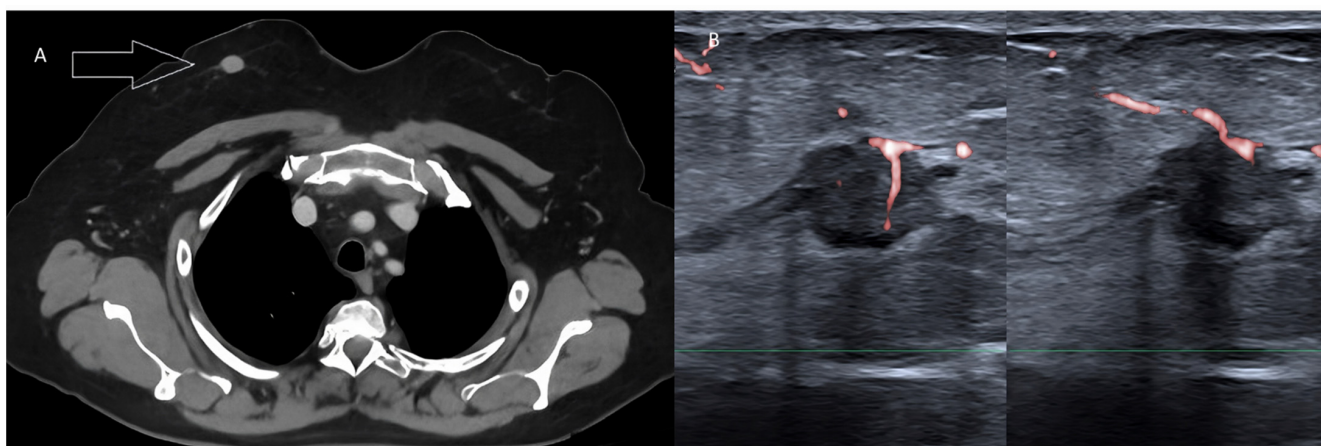


Figure 11. Pure tubular carcinoma detected incidentally during whole-body CT in a female patient with rectal cancer. (A) Contrast-enhanced, venous-phase CT scan detecting a nodule within the right breast (arrow). (B) Targeted US scan displaying the malignant lesion.

4. Conclusions—Not Everything That Glitters Is Gold

Despite the tremendous advances illustrated in this review, it is important to highlight a number of ongoing limitations and pitfalls. A large, fatty breast is still a problem for US scan, and US should never be employed as the only modality to evaluate such a case [11]. Microcalcification must be accurately detected and characterized, and this aspect is still a duty of mammography as US has limited sensitivity, especially when microcalcifications are not located inside a nodule. Moreover, a careful, multiparametric, US exam of the whole breasts and axillary cavities is time-consuming. Both in the case of sonographer-performed US and physician-performed US, this examination requires an adequate amount of time. Breast US should be carried out with top-level scanners, equipped with all the software capabilities allowing to perform a multiparametric investigation. Due to continuous direct contact with the patient and the high emotional involvement of women with any breast-related trouble, mammary US requires special abilities from the operator to concentrate and, at the same time, show good empathy [124–127]. Additionally, despite many attempts at methodological and lexical standardization and the introduction of ABUS, US is still a subjective exam that depends on the skills of the single operator, with limitations in terms of objectivity and intra-observer and inter-observer reproducibility.

Finally, it must be considered that competition from other imaging modalities is strong. As with US, mammography and MRI have also shown significant improvements through the years, and other techniques are being proposed as well [128,129]. Digital tomosynthesis and contrast-enhanced spectral mammography are quite important options, now employed routinely [82,98,130–132]. Quantitative perfusion MRI, MR lymphography, blood oxygenation level-dependent MRI, and diffusion-weighted MRI have all increased the impact of this modality [130–134]. However, it should always be kept in mind that all imaging modalities have their points of strength and weakness. Consequently, all modalities must be employed in the most appropriate way to cover the diagnostic needs of each single patient.

Author Contributions: O.C., R.F., F.D.M., I.S., P.P., F.B., A.B. (Alessandra Borgheresi), A.A., M.G., C.V., A.B. (Antonio Barile), A.G., N.G., V.M. and V.G. written and revised the manuscript. All authors have read and agreed to the published version of the manuscript.

Funding: This research received no external funding.

Institutional Review Board Statement: Not applicable.

Informed Consent Statement: Not applicable.

Data Availability Statement: All data are reported in the manuscript.

Acknowledgments: The authors are grateful to Alessandra Trocino, librarian at the National Cancer Institute of Naples, Italy.

Conflicts of Interest: The authors declare no conflict of interest.

References

1. Dodd, G.D. Present status of thermography, ultrasound and mammography in breast cancer detection. *Cancer* **1977**, *39*, 2796–2805. [[CrossRef](#)]
2. Sickles, E.A.; Filly, R.A.; Callen, P.W. Breast cancer detection with sonography and mammography: Comparison using state-of-the-art equipment. *Am. J. Roentgenol.* **1983**, *140*, 843–845. [[CrossRef](#)]
3. Dempsey, P.J. The History of Breast Ultrasound. *J. Ultrasound Med.* **2004**, *23*, 887–894. [[CrossRef](#)]
4. Agarwal, M.; van der Pol, C.B.; Patlas, M.N.; Udare, A.; Chung, A.D.; Rubino, J. Optimizing the radiologist work environment: Actionable tips to improve workplace satisfaction, efficiency, and minimize burnout. *Radiol. Med.* **2021**, *126*, 1255–1257. [[CrossRef](#)] [[PubMed](#)]
5. Albano, D.; Stecco, A.; Micci, G.; Sconfienza, L.M.; Colagrande, S.; Reginelli, A.; Grassi, R.; Carriero, A.; Midiri, M.; Lagalla, R.; et al. Whole-body magnetic resonance imaging (WB-MRI) in oncology: An Italian survey. *Radiol. Med.* **2020**, *126*, 299–305. [[CrossRef](#)] [[PubMed](#)]
6. Ahmed, S.A.; Samy, M.; Ali, A.M.; Hassan, R.A. Architectural distortion outcome: Digital breast tomosynthesis-detected versus digital mammography-detected. *Radiol. Med.* **2021**, *127*, 30–38. [[CrossRef](#)] [[PubMed](#)]
7. Argalia, G.; Ventura, C.; Tosi, N.; Campioni, D.; Tagliati, C.; Tuffaro, M.; Cucco, M.; Svegliati Baroni, G.; Giovagnoni, A. Comparison of point shear wave elastography and transient elastography in the evaluation of patients with NAFLD. *Radiol. Med.* **2022**, *127*, 571–576. [[CrossRef](#)]
8. Argalia, G.; Tarantino, G.; Ventura, C.; Campioni, D.; Tagliati, C.; Guardati, P.; Kostandini, A.; Marzoni, M.; Giuseppetti, G.M.; Giovagnoni, A. Shear wave elastography and transient elastography in HCV patients after direct-acting antivirals. *Radiol. Med.* **2021**, *126*, 894–899. [[CrossRef](#)] [[PubMed](#)]
9. Grani, G.; Lamartina, L.; Biffoni, M.; Giacomelli, L.; Maranghi, M.; Falcone, R.; Ramundo, V.; Cantisani, V.; Filetti, S.; Durante, C. Sonographically Estimated Risks of Malignancy for Thyroid Nodules Computed with Five Standard Classification Systems: Changes over Time and Their Relation to Malignancy. *Thyroid* **2018**, *28*, 1190–1197. [[CrossRef](#)]
10. American College of Radiology ACR-BI-RADS-Ultrasound. *ACR Breast Imaging Reporting and Data System, Breast Imaging Atlas*; American College of Radiology: Reston, VA, USA, 2003.
11. Hooley, R.J.; Scoutt, L.M.; Philpotts, L.E. Breast ultrasonography: State of the art. *Radiology* **2013**, *268*, 642–659. [[CrossRef](#)]
12. Brizi, M.G.; Perillo, F.; Cannone, F.; Tuzza, L.; Manfredi, R. The role of imaging in acute pancreatitis. *Radiol. Med.* **2021**, *126*, 1017–1029. [[CrossRef](#)] [[PubMed](#)]
13. Catalano, O.; Wortsman, X. Dermatology ultrasound. imaging technique, tips and tricks, high-resolution anatomy. *Ultrasound Q.* **2020**, *36*, 321–327. [[CrossRef](#)] [[PubMed](#)]
14. Catalano, O.; Varelli, C.; Sbordone, C.; Corvino, A.; De Rosa, D.; Vallone, G.; Wortsman, X. A bump: What to do next? ultrasound imaging of superficial soft-tissue palpable lesions. *J. Ultrasound* **2020**, *23*, 287–300. [[CrossRef](#)]
15. Catalano, O.; Mattace Raso, M.; D’Aiuto, M.; Illiano, L.A.; Saturnino, P.P.; Siani, A. Additional role of colour Doppler ultrasound imaging in intracystic breast tumours. *Radiol. Med.* **2009**, *114*, 253–266. [[CrossRef](#)] [[PubMed](#)]
16. Chang, R.F.; Huang, S.F.; Moon, W.K.; Lee, Y.H.; Chen, D.R. Solid Breast Masses: Neural Network Analysis of Vascular Features at Three-dimensional Power Doppler US for Benign or Malignant Classification. *Radiology* **2007**, *243*, 56–62. [[CrossRef](#)]
17. Chiti, G.; Grazzini, G.; Flammia, F.; Matteuzzi, B.; Tortoli, P.; Bettarini, S.; Pasqualini, E.; Granata, V.; Busoni, S.; Messerini, L.; et al. Gastroenteropancreatic neuroendocrine neoplasms (GEP-NENs): A radiomic model to predict tumor grade. *Radiol. Med.* **2022**, *127*, 928–938. [[CrossRef](#)]
18. Di Serafino, M.; Vallone, G. The role of point of care ultrasound in radiology department: Update and prospective. A statement of Italian college ultrasound. *Radiol. Med.* **2021**, *126*, 636–641. [[CrossRef](#)]
19. Horvath, E.; Cuitiño, M.J.; Pinochet, M.A.; Sanhueza, P. Color Doppler in the study of the breast: How do we perform it? *Rev. Chil. Radiol.* **2011**, *17*, 19–27.
20. Granata, V.; Simonetti, I.; Fusco, R.; Setola, S.V.; Izzo, F.; Scarpato, L.; Vanella, V.; Festino, L.; Simeone, E.; Ascierio, P.A.; et al. Management of cutaneous melanoma: Radiologists challenging and risk assessment. *Radiol. Med.* **2022**, *127*, 899–911. [[CrossRef](#)]
21. Granata, V.; Faggioni, L.; Grassi, R.; Fusco, R.; Reginelli, A.; Rega, D.; Maggioletti, N.; Buccicardi, D.; Frittoli, B.; Rengo, M.; et al. Structured reporting of computed tomography in the staging of colon cancer: A Delphi consensus proposal. *Radiol. Med.* **2022**, *127*, 21–29. [[CrossRef](#)]
22. Granata, V.; Grassi, R.; Fusco, R.; Setola, S.V.; Belli, A.; Ottaiano, A.; Nasti, G.; La Porta, M.; Danti, G.; Cappabianca, S.; et al. Intrahepatic cholangiocarcinoma and its differential diagnosis at MRI: How radiologist should assess MR features. *Radiol. Med.* **2021**, *126*, 1584–1600. [[CrossRef](#)] [[PubMed](#)]
23. Cappabianca, S.; Granata, V.; Di Grezia, G.; Mandato, Y.; Reginelli, A.; Di Mizio, V.; Grassi, R.; Rotondo, A. The role of nasoenteric intubation in the MR study of patients with Crohn’s disease: Our experience and literature review. *Radiol. Med.* **2010**, *116*, 389–406, English, Italian. [[CrossRef](#)]

24. Granata, V.; Fusco, R.; De Muzio, F.; Cutolo, C.; Setola, S.V.; Grassi, R.; Grassi, F.; Ottaiano, A.; Nasti, G.; Tatangelo, F.; et al. Radiomics textural features by MR imaging to assess clinical outcomes following liver resection in colorectal liver metastases. *Radiol. Med.* **2022**, *127*, 461–470. [[CrossRef](#)] [[PubMed](#)]
25. Granata, V.; Fusco, R.; De Muzio, F.; Cutolo, C.; Setola, S.V.; Dell'Aversana, F.; Grassi, F.; Belli, A.; Silvestro, L.; Ottaiano, A.; et al. Radiomics and machine learning analysis based on magnetic resonance imaging in the assessment of liver mucinous colorectal metastases. *Radiol. Med.* **2022**, *127*, 763–772. [[CrossRef](#)]
26. Sansone, M.; Marrone, S.; Di Salvio, G.; Belfiore, M.P.; Gatta, G.; Fusco, R.; Vanore, L.; Zuiani, C.; Grassi, F.; Vietri, M.T.; et al. Comparison between two packages for pectoral muscle removal on mammographic images. *Radiol. Med.* **2022**, *127*, 848–856. [[CrossRef](#)]
27. Gabelloni, M.; Faggioni, L.; Cioni, D.; Mendola, V.; Falaschi, Z.; Coppola, S.; Corradi, F.; Isirdi, A.; Brandi, N.; Coppola, F.; et al. Extracorporeal membrane oxygenation (ECMO) in COVID-19 patients: A pocket guide for radiologists. *Radiol. Med.* **2022**, *127*, 369–382. [[CrossRef](#)]
28. Ossola, C.; Curti, M.; Calvi, M.; Tack, S.; Mazzoni, S.; Genesio, L.; Venturini, M.; Genovese, E.A. Role of ultrasound and magnetic resonance imaging in the prognosis and classification of muscle injuries in professional football players: Correlation between imaging and return to sport time. *Radiol. Med.* **2021**, *126*, 1460–1467. [[CrossRef](#)] [[PubMed](#)]
29. Bakdik, S.; Arslan, S.; Oncu, F.; Durmaz, M.S.; Altunkeser, A.; Eryilmaz, M.A.; Unlu, Y. Effectiveness of Superb Microvascular Imaging for the differentiation of intraductal breast lesions. *Med Ultrason.* **2018**, *20*, 306–312. [[CrossRef](#)]
30. Cai, S.-M.; Wang, H.-V.; Zhang, X.-Y.; Zhang, L.; Zhu, Q.-L.; Li, J.-C.; Sun, Q.; Jiang, Y.-X. The Vascular Index of Superb Microvascular Imaging Can Improve the Diagnostic Accuracy for Breast Imaging Reporting and Data System Category 4 Breast Lesions. *Cancer Manag. Res.* **2020**, *12*, 1819–1826. [[CrossRef](#)]
31. Corvino, A.; Varelli, C.; Cocco, G.; Corvino, F.; Catalano, O. Seeing the unseen with superb microvascular imaging: Ultrasound depiction of normal dermis vessels. *J. Clin. Ultrasound* **2022**, *50*, 121–127. [[CrossRef](#)]
32. Corvino, A.; Varelli, C.; Catalano, F.; Cocco, G.; Delli Pizzi, A.; Boccatonda, A.; Corvino, F.; Basile, L.; Catalano, O. Use of high-frequency transducers in breast sonography. *J. Pers. Med.* **2022**, *12*, 1960. [[CrossRef](#)]
33. Corvino, A.; Catalano, O.; Varelli, C.; Cocco, G.; Delli Pizzi, A.; Corvino, F.; Tafuri, D.; Caruso, M. Non-glandular findings on breast ultrasound. Part II: A pictorial review of chest wall lesions. *J. Ultrasound* **2023**, 1–10. [[CrossRef](#)] [[PubMed](#)]
34. Kim, S.; Lee, H.J.; Ko, K.H.; Park, A.Y.; Koh, J.; Jung, H.K. New Doppler imaging technique for assessing angiogenesis in breast tumors: Correlation with immunohistochemically analyzed microvessels density. *Acta Radiol.* **2018**, *59*, 1414–1421. [[CrossRef](#)]
35. Park, A.Y.; Seo, B.K. Up-to-date Doppler techniques for breast tumor vascularity: Superb microvascular imaging and contrast-enhanced ultrasound. *Ultrasonography* **2018**, *37*, 98–106. [[CrossRef](#)]
36. Park, A.Y.; Kwon, M.; Woo, O.H.; Cho, K.R.; Park, E.K.; Cha, S.H.; Song, S.E.; Lee, J.-H.; Cha, J.; Son, G.S.; et al. A Prospective Study on the Value of Ultrasound Microflow Assessment to Distinguish Malignant from Benign Solid Breast Masses: Association between Ultrasound Parameters and Histologic Microvessel Densities. *Korean J. Radiol.* **2019**, *20*, 759–772. [[CrossRef](#)] [[PubMed](#)]
37. Zhu, Y.-C.; Zhang, Y.; Deng, S.-H.; Jiang, Q. Diagnostic Performance of Superb Microvascular Imaging (SMI) Combined with Shear-Wave Elastography in Evaluating Breast Lesions. *Experiment* **2018**, *24*, 5935–5942. [[CrossRef](#)]
38. BBarile, A. Correction to: Some thoughts and greetings from the new Editor-in-Chief. *Radiol. Med.* **2021**, *126*, 1377. [[CrossRef](#)]
39. Catalano, O.; Corvino, A.; Basile, L.; Catalano, F.; Varelli, C. Use of new microcirculation software allows the demonstration of dermis vascularization. *J. Ultrasound* **2022**, 1–6. [[CrossRef](#)]
40. Sivakumar, L.; Alturkistani, H.; Lerouge, S.; Bertrand-Grenier, A.; Zehtabi, F.; Thérèse, É.; Roy-Cardinal, M.-H.; Bhatnagar, S.; Cloutier, G.; Soulez, G. Strain Ultrasound Elastography of Aneurysm Sac Content after Randomized Endoleak Embolization with Sclerosing vs. Non-sclerosing Chitosan-based Hydrogels in a Canine Model. *J. Vasc. Interv. Radiol.* **2022**, *33*, 495–504. [[CrossRef](#)] [[PubMed](#)]
41. Bartolotta, T.V.; Orlando, A.A.M.; Dimarco, M.; Zarcaro, C.; Ferraro, F.; Cirino, A.; Matranga, D.; Vieni, S.; Cabibi, D. Diagnostic performance of 2D-shear wave elastography in the diagnosis of breast cancer: A clinical appraisal of cutoff values. *Radiol. Med.* **2022**, *127*, 1209–1220. [[CrossRef](#)]
42. Ding, S.-S.; Liu, C.; Zhang, Y.-F.; Sun, L.-P.; Xiang, L.-H.; Liu, H.; Fang, Y.; Ren, W.-W.; Zhao, H.; Sun, X.-M.; et al. Contrast-enhanced ultrasound in the assessment of Crohn's disease activity: Comparison with computed tomography enterography. *Radiol. Med.* **2022**, *127*, 1068–1078. [[CrossRef](#)]
43. Elia, D.; Fresilli, D.; Pacini, P.; Cardaccio, S.; Polti, G.; Guiban, O.; Celletti, I.; Kutrolli, E.; De Felice, C.; Occhiato, R.; et al. Can strain US-elastography with strain ratio (SRE) improve the diagnostic accuracy in the assessment of breast lesions? Preliminary results. *J. Ultrasound* **2020**, *24*, 157–163. [[CrossRef](#)]
44. Hyodo, R.; Takehara, Y.; Naganawa, S. 4D Flow MRI in the portal venous system: Imaging and analysis methods, and clinical applications. *Radiol. Med.* **2022**, *127*, 1181–1198. [[CrossRef](#)]
45. Ruan, S.-M.; Huang, H.; Cheng, M.-Q.; Lin, M.-X.; Hu, H.-T.; Huang, Y.; Li, M.-D.; Wang, W. Shear-wave elastography combined with contrast-enhanced ultrasound algorithm for noninvasive characterization of focal liver lesions. *Radiol. Med.* **2022**, 1–10. [[CrossRef](#)] [[PubMed](#)]
46. Ruscitti, P.; Esposito, M.; Gianneramo, C.; Di Cola, I.; De Berardinis, A.; Martinese, A.; Tochap, G.N.; Conforti, A.; Masciocchi, C.; Cipriani, P.; et al. Nail and entheses assessment in patients with psoriatic disease by high frequency ultrasonography: Findings from a single-centre cross-sectional study. *Radiol. Med.* **2022**, *127*, 1400–1406. [[CrossRef](#)] [[PubMed](#)]

47. Salaffi, F.; Carotti, M.; Di Matteo, A.; Ceccarelli, L.; Farah, S.; Villota-Eraso, C.; Di Carlo, M.; Giovagnoni, A. Ultrasound and magnetic resonance imaging as diagnostic tools for sarcopenia in immune-mediated rheumatic diseases (IMRDs). *Radiol. Med.* **2022**, *127*, 1277–1291. [[CrossRef](#)] [[PubMed](#)]
48. Ventura, C.; Baldassarre, S.; Cerimele, F.; Pepi, L.; Marconi, E.; Ercolani, P.; Floridi, C.; Argalia, G.; Goteri, G.; Giovagnoni, A. 2D shear wave elastography in evaluation of prognostic factors in breast cancer. *Radiol. Med.* **2022**, *127*, 1221–1227. [[CrossRef](#)]
49. Youk, J.H.; Gweon, H.M.; Son, E.J. Shear-wave elastography in breast ultrasonography: The state of the art. *Ultrasonography* **2017**, *36*, 300–309. [[CrossRef](#)]
50. Barr, R.G.; Nakashima, K.; Amy, D.; Cosgrove, D.; Farrokh, A.; Schafer, F.; Bamber, J.C.; Castera, L.; Choi, B.I.; Chou, Y.-H.; et al. WFUMB guidelines and recommendations for clinical use of ultrasound elastography: Part 2, breast. *Ultrasound Med. Biol.* **2015**, *41*, 1148–1160. [[CrossRef](#)]
51. Barr, R.G. Future of breast elastography. *Ultrasonography* **2019**, *38*, 93–105. [[CrossRef](#)]
52. Luo, S.; Yao, G.; Hong, Z.; Zhang, S.; Wang, W.; Zhang, J.; Zhang, Y.; Wu, J.; Zhang, L.; Cheng, H.; et al. Qualitative Classification of Shear Wave Elastography for Differential Diagnosis Between Benign and Metastatic Axillary Lymph Nodes in Breast Cancer. *Front. Oncol.* **2019**, *9*, 533. [[CrossRef](#)] [[PubMed](#)]
53. Lee, S.H.; Chang, J.M.; Cho, N.; Koo, H.R.; Yi, A.; Kim, S.J.; Youk, J.H.; Son, E.J.; Choi, S.H.; Kook, S.H.; et al. Practice guideline for the performance of breast ultrasound elastography. *Ultrasonography* **2013**, *33*, 3–10. [[CrossRef](#)]
54. Sezgin, G.; Coskun, M.; Apaydin, M.; Sari, A.A. The role of rare breast cancers in the false negative strain elastography results. *Radiol. Med.* **2021**, *126*, 349–355. [[CrossRef](#)] [[PubMed](#)]
55. Trombadori, C.M.L.; D’Angelo, A.; Ferrara, F.; Santoro, A.; Belli, P.; Manfredi, R. Radial Scar: A management dilemma. *Radiol. Med.* **2021**, *126*, 774–785. [[CrossRef](#)]
56. Kapetas, P.; Woitek, R.; Clauser, P.; Bernathova, M.; Pinker, K.; Helbich, T.H.; Baltzer, P.A. A Simple Ultrasound Based Classification Algorithm Allows Differentiation of Benign from Malignant Breast Lesions by Using Only Quantitative Parameters. *Mol. Imaging Biol.* **2018**, *20*, 1053–1060. [[CrossRef](#)]
57. De Muzio, F.; Grassi, F.; Dell’Aversana, F.; Fusco, R.; Danti, G.; Flammia, F.; Chiti, G.; Valeri, T.; Agostini, A.; Palumbo, P.; et al. A Narrative Review on LI-RADS Algorithm in Liver Tumors: Prospects and Pitfalls. *Diagnostics* **2022**, *12*, 1655. [[CrossRef](#)]
58. Catalano, O.; Sandomenico, F.; Vallone, P.; Setola, S.V.; Granata, V.; Fusco, R.; Lastoria, S.; Mansi, L.; Petrillo, A. Contrast-Enhanced Ultrasound in the Assessment of Patients with Indeterminate Abdominal Findings at Positron Emission Tomography Imaging. *Ultrasound Med. Biol.* **2016**, *42*, 2717–2723. [[CrossRef](#)]
59. Granata, V.; Grassi, R.; Fusco, R.; Setola, S.; Belli, A.; Piccirillo, M.; Pradella, S.; Giordano, M.; Cappabianca, S.; Brunese, L.; et al. Abbreviated MRI Protocol for the Assessment of Ablated Area in HCC Patients. *Int. J. Environ. Res. Public Heal.* **2021**, *18*, 3598. [[CrossRef](#)] [[PubMed](#)]
60. Barretta, M.L.; Catalano, O.; Setola, S.V.; Granata, V.; Marone, U.; Gallipoli, A.D. Gallbladder metastasis: Spectrum of imaging findings. *Abdom. Imaging* **2011**, *36*, 729–734. [[CrossRef](#)]
61. Granata, V.; Fusco, R.; Catalano, O.; Avallone, A.; Palaia, R.; Botti, G.; Tatangelo, F.; Granata, F.; Cascella, M.; Izzo, F.; et al. Diagnostic accuracy of magnetic resonance, computed tomography and contrast enhanced ultrasound in radiological multimodality assessment of peribiliary liver metastases. *PLoS ONE* **2017**, *12*, e0179951. [[CrossRef](#)]
62. Granata, V.; Castelguidone, E.D.L.D.; Fusco, R.; Catalano, O.; Piccirillo, M.; Palaia, R.; Izzo, F.; Gallipoli, A.D.; Petrillo, A. Irreversible electroporation of hepatocellular carcinoma: Preliminary report on the diagnostic accuracy of magnetic resonance, computer tomography, and contrast-enhanced ultrasound in evaluation of the ablated area. *Radiol. Med.* **2015**, *121*, 122–131. [[CrossRef](#)] [[PubMed](#)]
63. Chou, C.-P.; Huang, J.-S.; Wang, J.-S.; Pan, H.-B. Contrast-enhanced ultrasound features of breast capillary hemangioma: A case report and review of literature. *J. Ultrasound* **2022**, *25*, 103–106. [[CrossRef](#)] [[PubMed](#)]
64. Guo, R.; Lu, G.; Qin, B.; Fei, B. Ultrasound Imaging Technologies for Breast Cancer Detection and Management: A Review. *Ultrasound Med. Biol.* **2018**, *44*, 37–70. [[CrossRef](#)]
65. Faccioli, N.; Santi, E.; Foti, G.; D’Onofrio, M. Cost-effectiveness analysis of including contrast-enhanced ultrasound in management of pancreatic cystic neoplasms. *Radiol. Med.* **2022**, *127*, 349–359. [[CrossRef](#)] [[PubMed](#)]
66. Fresilli, D.; Di Leo, N.; Martinelli, O.; Di Marzo, L.; Pacini, P.; Dolcetti, V.; Del Gaudio, G.; Canni, F.; Ricci, L.I.; De Vito, C.; et al. 3D-Arterial analysis software and CEUS in the assessment of severity and vulnerability of carotid atherosclerotic plaque: A comparison with CTA and histopathology. *Radiol. Med.* **2022**, *127*, 1254–1269. [[CrossRef](#)] [[PubMed](#)]
67. Sofia, C.; Solazzo, A.; Cattafi, A.; Chimenz, R.; Cicero, G.; Marino, M.A.; D’Angelo, T.; Manti, L.; Condorelli, E.; Ceravolo, G.; et al. Contrast-enhanced voiding urosonography in the assessment of vesical-ureteral reflux: The time has come. *Radiol. Med.* **2021**, *126*, 901–909. [[CrossRef](#)]
68. Varghese, B.A.; Lee, S.; Cen, S.; Talebi, A.; Mohd, P.; Stahl, D.; Perkins, M.; Desai, B.; Duddalwar, V.A.; Larsen, L.H. Characterizing breast masses using an integrative framework of machine learning and CEUS-based radiomics. *J. Ultrasound* **2022**, *25*, 699–708. [[CrossRef](#)]
69. Jia, K.; Li, L.; Wu, X.J.; Hao, M.J.; Xue, H.Y. Contrast-enhanced ultrasound for evaluating the pathologic response of breast cancer to neoadjuvant chemotherapy. *Medicine* **2019**, *98*, e14258. [[CrossRef](#)]
70. Bin, L.; Huihui, Y.; Weiping, Y.; Changyuan, W.; Qinghong, Q.; Weiyu, M. Value of three-dimensional ultrasound in differentiating malignant from benign breast tumors. A systematic review and meta-analysis. *Ultrasound Q.* **2019**, *35*, 68–73. [[CrossRef](#)]

71. Satake, H.; Ishigaki, S.; Ito, R.; Naganawa, S. Radiomics in breast MRI: Current progress toward clinical application in the era of artificial intelligence. *Radiol. Med.* **2021**, *127*, 39–56. [[CrossRef](#)] [[PubMed](#)]
72. Rossi, F.; Lambertini, M.; Brunetti, N.; De Giorgis, S.; Razeti, M.G.; Calabrese, M.; Tagliafico, A.S. Muscle mass loss in breast cancer patients of reproductive age (≤ 45 years) undergoing neoadjuvant chemotherapy. *Radiol. Med.* **2022**, 1–9. [[CrossRef](#)]
73. Fiaschetti, V.; Ubaldi, N.; De Fazio, S.; Ricci, A.; Maspes, F.; Cossu, E. Digital tomosynthesis spot view in architectural distortions: Outcomes in management and radiation dose. *Radiol. Med.* **2022**, 1–14. [[CrossRef](#)]
74. Clauser, P.; Londero, V.; Como, G.; Girometti, R.; Bazzocchi, M.; Zuiani, C. Comparison between different imaging techniques in the evaluation of malignant breast lesions: Can 3D ultrasound be useful? *Radiol. Med.* **2014**, *119*, 240–248. [[CrossRef](#)]
75. Park, A.Y.; Seo, B.K.; Cho, K.R.; Woo, O.H. The utility of MicroPure™ ultrasound technique in assessing grouped microcalcifications without a mass on mammography. *J. Breast Cancer* **2016**, *19*, 83–86. [[CrossRef](#)] [[PubMed](#)]
76. van Zelst, J.C.; Mann, R.M. Automated three-dimensional breast US for screening: Technique, artifacts, and lesion characterization. *Radio Graph.* **2018**, *38*, 663–683. [[CrossRef](#)]
77. Zanotel, M.; Bednarova, I.; Londero, V.; Linda, A.; Lorenzon, M.; Girometti, R.; Zuiani, C. Automated breast ultrasound: Basic principles and emerging clinical applications. *Radiol. Med.* **2018**, *123*, 1–12. [[CrossRef](#)] [[PubMed](#)]
78. Schiaffino, S.; Cristina, L.; Tosto, S.; Massone, E.; De Giorgis, S.; Garlaschi, A.; Tagliafico, A.; Calabrese, M. The value of coronal view as a stand-alone assessment in women undergoing automated breast ultrasound. *Radiol. Med.* **2020**, *126*, 206–213. [[CrossRef](#)] [[PubMed](#)]
79. Barr, R.G.; DeVita, R.; Destounis, S.; Manzoni, F.; De Silvestri, A.; Tinelli, C. Agreement between an automated volume breast scanner and hand held ultrasound for diagnostic breast examinations. *J. Ultrasound. Med.* **2017**, *36*, 2087–2092. [[CrossRef](#)]
80. Brem, R.F.; Tabár, L.; Duffy, S.W.; Inciardi, M.F.; Guingrich, J.A.; Hashimoto, B.E.; Lander, M.R.; Lapidus, R.L.; Peterson, M.K.; Rapelyea, J.A.; et al. Assessing Improvement in Detection of Breast Cancer with Three-dimensional Automated Breast US in Women with Dense Breast Tissue: The SomoInsight Study. *Radiology* **2015**, *274*, 663–673. [[CrossRef](#)]
81. D’Angelo, A.; Orlandi, A.; Bufi, E.; Mercogliano, S.; Belli, P.; Manfredi, R. Automated breast volume scanner (ABVS) compared to handheld ultrasound (HHUS) and contrast-enhanced magnetic resonance imaging (CE-MRI) in the early assessment of breast cancer during neoadjuvant chemotherapy: An emerging role to monitoring tumor response? *Radiol. Med.* **2021**, *126*, 517–526. [[CrossRef](#)] [[PubMed](#)]
82. Girometti, R.; Zanotel, M.; Londero, V.; Bazzocchi, M.; Zuiani, C. Comparison between automated breast volume scanner (ABVS) versus hand-held ultrasound as a second look procedure after magnetic resonance imaging. *Eur. Radiol.* **2017**, *27*, 3767–3775. [[CrossRef](#)]
83. Coppola, F.; Faggioni, L.; Regge, D.; Giovagnoni, A.; Golfieri, R.; Bibbolino, C.; Miele, V.; Neri, E.; Grassi, R. Artificial intelligence: Radiologists’ expectations and opinions gleaned from a nationwide online survey. *Radiol. Med.* **2021**, *126*, 63–71. [[CrossRef](#)] [[PubMed](#)]
84. Nardone, V.; Reginelli, A.; Grassi, R.; Boldrini, L.; Vacca, G.; D’Ippolito, E.; Annunziata, S.; Farchione, A.; Belfiore, M.P.; Desideri, I.; et al. Delta radiomics: A systematic review. *Radiol. Med.* **2021**, *126*, 1571–1583. [[CrossRef](#)]
85. Tadayyon, H.; Gangeh, M.; Sannachi, L.; Trudeau, M.; Pritchard, K.; Ghandi, S.; Eisen, A.; Look-Hong, N.; Holloway, C.; Wright, F.; et al. A priori prediction of breast tumour response to chemotherapy using quantitative ultrasound imaging and artificial neural networks. *Oncotarget* **2019**, *10*, 3910–3923. [[CrossRef](#)] [[PubMed](#)]
86. Vicini, S.; Bortolotto, C.; Rengo, M.; Ballerini, D.; Bellini, D.; Carbone, I.; Preda, L.; Laghi, A.; Coppola, F.; Faggioni, L. A narrative review on current imaging applications of artificial intelligence and radiomics in oncology: Focus on the three most common cancers. *Radiol. Med.* **2022**, *127*, 819–836. [[CrossRef](#)] [[PubMed](#)]
87. Simonetti, I.; Bruno, F.; Fusco, R.; Cutolo, C.; Setola, S.V.; Patrone, R.; Masciocchi, C.; Palumbo, P.; Arrigoni, F.; Picone, C.; et al. Multimodality Imaging Assessment of Desmoid Tumors: The Great Mime in the Era of Multidisciplinary Teams. *J. Pers. Med.* **2022**, *12*, 1153. [[CrossRef](#)]
88. Granata, V.; Fusco, R.; Avallone, A.; De Stefano, A.; Ottaiano, A.; Sbordone, C.; Brunese, L.; Izzo, F.; Petrillo, A. Radiomics-Derived Data by Contrast Enhanced Magnetic Resonance in RAS Mutations Detection in Colorectal Liver Metastases. *Cancers* **2021**, *13*, 453. [[CrossRef](#)]
89. Granata, V.; Fusco, R.; Risi, C.; Ottaiano, A.; Avallone, A.; De Stefano, A.; Grimm, R.; Grassi, R.; Brunese, L.; Izzo, F.; et al. Diffusion-Weighted MRI and Diffusion Kurtosis Imaging to Detect RAS Mutation in Colorectal Liver Metastasis. *Cancers* **2020**, *12*, 2420. [[CrossRef](#)]
90. Wilding, R.; Sheraton, V.M.; Soto, L.; Chotai, N.; Tan, E.Y. Deep learning applied to breast imaging classification and segmentation with human expert intervention. *J. Ultrasound* **2022**, *25*, 659–666. [[CrossRef](#)]
91. Cirtsis, A.; Rossi, C.; Eberhard, M.; Marcon, M.; Becker, A.S.; Boss, A. Automatic classification of ultrasound breast lesions using a deep convolutional neural network mimicking human decision-making. *Eur. Radiol.* **2019**, *29*, 5458–5468. [[CrossRef](#)]
92. Zeng, D.; Xu, M.; Liang, J.-Y.; Cheng, M.-Q.; Huang, H.; Pan, J.-M.; Huang, Y.; Tong, W.-J.; Xie, X.-Y.; Lu, M.-D.; et al. Using new criteria to improve the differentiation between HCC and non-HCC malignancies: Clinical practice and discussion in CEUS LI-RADS 2017. *Radiol. Med.* **2021**, *127*, 1–10. [[CrossRef](#)] [[PubMed](#)]
93. Jiang, M.; Li, C.-L.; Luo, X.-M.; Chuan, Z.-R.; Lv, W.-Z.; Li, X.; Cui, X.-W.; Dietrich, C.F. Ultrasound-based deep learning radiomics in the assessment of pathological complete response to neoadjuvant chemotherapy in locally advanced breast cancer. *Eur. J. Cancer* **2021**, *147*, 95–105. [[CrossRef](#)] [[PubMed](#)]

94. Ilesanmi, A.E.; Chaumrattanakul, U.; Makhanov, S.S. Methods for the segmentation and classification of breast ultrasound images: A review. *J. Ultrasound* **2021**, *24*, 367–382. [[CrossRef](#)]
95. Scapicchio, C.; Gabelloni, M.; Barucci, A.; Cioni, D.; Saba, L.; Neri, E. A deep look into radiomics. *Radiol. Med.* **2021**, *126*, 1296–1311. [[CrossRef](#)] [[PubMed](#)]
96. Wu, G.-G.; Zhou, L.-Q.; Xu, J.-W.; Wang, J.-Y.; Wei, Q.; Deng, Y.-B.; Cui, X.-W.; Dietrich, C.F. Artificial intelligence in breast ultrasound. *World J. Radiol.* **2019**, *11*, 19–26. [[CrossRef](#)] [[PubMed](#)]
97. Bartolotta, T.V.; Orlando, A.; Cantisani, V.; Matranga, D.; Ienzi, R.; Cirino, A.; Amato, F.; Di Vittorio, M.L.; Midiri, M.; Lagalla, R. Focal breast lesion characterization according to the BI-RADS US lexicon: Role of a computer-aided decision-making support. *Radiol. Med.* **2018**, *123*, 498–506. [[CrossRef](#)] [[PubMed](#)]
98. Bartolotta, T.V.; Orlando, A.A.M.; Spatafora, L.; Dimarco, M.; Gagliardo, C.; Taibbi, A. S-Detect characterization of focal breast lesions according to the US BI RADS lexicon: A pictorial essay. *J. Ultrasound* **2020**, *23*, 207–215. [[CrossRef](#)]
99. Bartolotta, T.V.; Orlando, A.A.M.; Di Vittorio, M.L.; Amato, F.; Dimarco, M.; Matranga, D.; Ienzi, R. S-Detect characterization of focal solid breast lesions: A prospective analysis of inter-reader agreement for US BI-RADS descriptors. *J. Ultrasound* **2020**, *24*, 143–150. [[CrossRef](#)]
100. Zhao, C.; Xiao, M.; Jiang, Y.; Liu, H.; Wang, M.; Wang, H.; Sun, Q.; Zhu, Q. Feasibility of computer-assisted diagnosis for breast ultrasound: The results of the diagnostic performance of S-detect from a single center in China. *Cancer Manag. Res.* **2019**, *11*, 921–930. [[CrossRef](#)]
101. Di Segni, M.; de Soccio, V.; Cantisani, V.; Bonito, G.; Rubini, A.; Di Segni, G.; Lamorte, S.; Magri, V.; De Vito, C.; Migliara, G.; et al. Automated classification of focal breast lesions according to S-detect: Validation and role as a clinical and teaching tool. *J. Ultrasound* **2018**, *21*, 105–118. [[CrossRef](#)]
102. Chiao, J.-Y.; Chen, K.-Y.; Liao, K.Y.-K.; Hsieh, P.-H.; Zhang, G.; Huang, T.-C. Detection and classification the breast tumors using mask R-CNN on sonograms. *Medicine* **2019**, *98*, e15200. [[CrossRef](#)]
103. Gao, Y.; Luo, Y.; Zhao, C.; Xiao, M.; Ma, L.; Li, W.; Qin, J.; Zhu, Q.; Jiang, Y. Nomogram based on radiomics analysis of primary breast cancer ultrasound images: Prediction of axillary lymph node tumor burden in patients. *Eur. Radiol.* **2021**, *31*, 928–937. [[CrossRef](#)] [[PubMed](#)]
104. Fausto, A.; Rizzato, G.; Preziosa, A.; Gaburro, L.; Washburn, M.J.; Rubello, D.; Volterrani, L. A new method to combine contrast-enhanced magnetic resonance imaging during live ultrasound of the breast using volume navigation technique: A study for evaluating feasibility, accuracy and reproducibility in healthy volunteers. *Eur. J. Radiol.* **2012**, *81*, e332–e337. [[CrossRef](#)]
105. Kucukkaya, F.; Aribal, E.; Tureli, D.; Altas, H.; Kaya, H. Use of a Volume Navigation Technique for Combining Real-Time Ultrasound and Contrast-Enhanced MRI: Accuracy and Feasibility of a Novel Technique for Locating Breast Lesions. *Am. J. Roentgenol.* **2016**, *206*, 217–225. [[CrossRef](#)]
106. Papalexis, N.; Parmeggiani, A.; Facchini, G.; Miceli, M.; Carbone, G.; Cavallo, M.; Spinnato, P. Current concepts in the diagnosis and treatment of adhesive capsulitis: Role of diagnostic imaging and ultrasound-guided interventional procedures. *Radiol. Med.* **2022**, *127*, 1390–1399. [[CrossRef](#)]
107. Crisan, D.; Wortsman, X.; Alfageme, F.; Catalano, O.; Badea, A.; Scharffetter-Kochanek, K.; Sindrilaru, A.; Crisan, M. Ultrasonography in dermatologic surgery: Revealing the unseen for improved surgical planning. *JDDG J. der Dtsch. Dermatol. Ges.* **2022**, *20*, 913–926. [[CrossRef](#)] [[PubMed](#)]
108. Moschetta, M.; Sardaro, A.; Nitti, A.; Telegrafo, M.; Maggialelli, N.; Scardapane, A.; Brunese, M.C.; Lavelli, V.; Ferrari, C. Ultrasound evaluation of ductal carcinoma in situ of the breast. *J. Ultrasound* **2021**, *25*, 41–45. [[CrossRef](#)] [[PubMed](#)]
109. Stavros, A.T.; Thickman, D.; Rapp, C.L.; Dennis, M.A.; Parker, S.H.; Sisney, G.A. Solid breast nodules: Use of sonography to distinguish between benign and malignant lesions. *Radiology* **1995**, *196*, 123–134. [[CrossRef](#)]
110. Deandrea, S.; Cavazzana, L.; Principi, N.; Luconi, E.; Campoleoni, M.; Bastiampillai, A.J.; Bracchi, L.; Bucchi, L.; Pedilarco, S.; Piscitelli, A.; et al. Screening of women with aesthetic prostheses in dedicated sessions of a population-based breast cancer screening programme. *Radiol. Med.* **2021**, *126*, 946–955. [[CrossRef](#)]
111. Fusco, R.; Petrillo, A.; Catalano, O.; Sansone, M.; Granata, V.; Filice, S.; D’Aiuto, M.; Pankhurst, Q.; Douek, M. Procedures for location of non-palpable breast lesions: A systematic review for the radiologist. *Breast Cancer* **2014**, *21*, 522–531. [[CrossRef](#)]
112. Nori, J.; Bicchierai, G.; Amato, F.; De Benedetto, D.; Boeri, C.; Vanzi, E.; Di Naro, F.; Bianchi, S.; Miele, V. A new technique for the histological diagnosis of Paget’s disease of the breast using a semiautomated core needle biopsy with a 14-gauge needle. *Radiol. Med.* **2021**, *126*, 936–945. [[CrossRef](#)] [[PubMed](#)]
113. Panzironi, G.; Moffa, G.; Galati, F.; Pediconi, F. Ultrasound-guided 8-Gauge vacuum-assisted excision for selected B3 breast lesions: A preliminary experience. *Radiol. Med.* **2022**, *127*, 57–64. [[CrossRef](#)] [[PubMed](#)]
114. Petrillo, A.; Di Giacomo, R.; Esposito, E.; Vallone, P.; Setola, S.V.; Raso, M.M.; Granata, V.; Barretta, M.L.; Siani, C.; Rinaldo, C.; et al. Preoperative localisation of nonpalpable breast lesions using magnetic markers in a tertiary cancer centre. *Eur. Radiol. Exp.* **2022**, *6*, 28. [[CrossRef](#)]
115. Bellardita, L.; Colciago, R.R.; Frasca, S.; De Santis, M.C.; Gay, S.; Palorini, F.; La Rocca, E.; Valdagni, R.; Rancati, T.; Lozza, L. Breast cancer patient perspective on opportunities and challenges of a genetic test aimed to predict radio-induced side effects before treatment: Analysis of the Italian branch of the REQUITE project. *Radiol. Med.* **2021**, *126*, 1366–1373. [[CrossRef](#)]

116. Carbonaro, L.A.; Rizzo, S.S.; Schiaffino, S.; Mainini, A.P.; Berger, N.; Trimboli, R.M.; Sardanelli, F. Biennial screening mammography: How many women ask for more? Estimate of the interval mammogram rate in an organised population-based screening programme. *Radiol. Med.* **2021**, *126*, 200–205. [[CrossRef](#)]
117. Caruso, M.; Catalano, O.; Bard, R.; Varelli, C.; Corvino, F.; Caiazzo, C.; Corvino, A. Non-glandular findings on breast ultrasound. Part I: A pictorial review of superficial lesions. *J. Ultrasound* **2022**, *25*, 783–797. [[CrossRef](#)] [[PubMed](#)]
118. Maio, F.; Tari, D.U.; Granata, V.; Fusco, R.; Grassi, R.; Petrillo, A.; Pinto, F. Breast Cancer Screening during COVID-19 Emergency: Patients and Department Management in a Local Experience. *J. Pers. Med.* **2021**, *11*, 380. [[CrossRef](#)]
119. Neri, E.; Granata, V.; Montemezzi, S.; Belli, P.; Bernardi, D.; Brancato, B.; Caumo, F.; Calabrese, M.; Coppola, F.; Cossu, E.; et al. Structured reporting of x-ray mammography in the first diagnosis of breast cancer: A Delphi consensus proposal. *Radiol. Med.* **2022**, *127*, 471–483. [[CrossRef](#)]
120. Deandrea, S.; Sardanelli, F.; Calabrese, M.; Ferré, F.; Vainieri, M.; Sestini, E.; Caumo, F.; Saguatti, G.; Bucchi, L.; Cataliotti, L. Provision of follow-up care for women with a history of breast cancer following the 2016 position paper by the Italian Group for Mammographic Screening and the Italian College of Breast Radiologists by SIRM: A survey of Senonetwork Italian breast centres. *Radiol. Med.* **2022**, *127*, 484–489. [[CrossRef](#)] [[PubMed](#)]
121. Granata, V.; Bicchierai, G.; Fusco, R.; Cozzi, D.; Grazzini, G.; Danti, G.; De Muzio, F.; Maggialetti, N.; Smorchkova, O.; D’Elia, M.; et al. Diagnostic protocols in oncology: Workup and treatment planning. Part 2: Abbreviated MR protocol. *Eur. Rev. Med. Pharmacol. Sci.* **2021**, *25*, 6499–6528. [[CrossRef](#)]
122. Leung, J.W. Second-look ultrasound: Only for biopsy or more? *Eur. J. Radiol.* **2012**, *81*, s87–s89. [[CrossRef](#)] [[PubMed](#)]
123. Sansone, M.; Grassi, R.; Belfiore, M.P.; Gatta, G.; Grassi, F.; Pinto, F.; La Casella, G.V.; Fusco, R.; Cappabianca, S.; Granata, V. Radiomic features of breast parenchyma: Assessing differences between FOR PROCESSING and FOR PRESENTATION digital mammography. *Insights Into Imaging* **2021**, *12*, 147. [[CrossRef](#)]
124. Fusco, R.; Granata, V.; Pariante, P.; Cerciello, V.; Siani, C.; Di Bonito, M.; Valentino, M.; Sansone, M.; Botti, G.; Petrillo, A. Blood oxygenation level dependent magnetic resonance imaging and diffusion weighted MRI imaging for benign and malignant breast cancer discrimination. *Magn. Reson. Imaging* **2020**, *75*, 51–59. [[CrossRef](#)] [[PubMed](#)]
125. Fusco, R.; Granata, V.; Raso, M.M.; Vallone, P.; De Rosa, A.; Siani, C.; Di Bonito, M.; Petrillo, A.; Sansone, M. Blood Oxygenation Level Dependent Magnetic Resonance Imaging (MRI), Dynamic Contrast Enhanced MRI, and Diffusion Weighted MRI for Benign and Malignant Breast Cancer Discrimination: A Preliminary Experience. *Cancers* **2021**, *13*, 2421. [[CrossRef](#)] [[PubMed](#)]
126. Girometti, R.; Linda, A.; Conte, P.; Lorenzon, M.; De Serio, I.; Jerman, K.; Londero, V.; Zuiani, C. Multireader comparison of contrast-enhanced mammography versus the combination of digital mammography and digital breast tomosynthesis in the preoperative assessment of breast cancer. *Radiol. Med.* **2021**, *126*, 1407–1414. [[CrossRef](#)]
127. Catalano, O.; Raso, M.M.; Petrillo, A.; D’Errico, A.G. Extended field of view in breast sonography. *Ultraschall Med* **2011**, *32*, 198–202. [[CrossRef](#)] [[PubMed](#)]
128. Petralia, G.; Zugni, F.; Summers, P.E.; Colombo, A.; Pricolo, P.; Grazioli, L.; Colagrande, S.; Giovagnoni, A.; Padhani, A.R.; On behalf of the Italian Working Group on Magnetic Resonance. Whole-body magnetic resonance imaging (WB-MRI) for cancer screening: Recommendations for use. *Radiol. Med.* **2021**, *126*, 1434–1450. [[CrossRef](#)]
129. Petrillo, A.; Catalano, O.; Fusco, R.; Filice, S.; Vallone, P.; Setola, S.; Granata, V.; Raiano, C.; Avino, F.; Di Bonito, M.; et al. Optical imaging of the breast: Evaluation of deoxyhemoglobin concentration alteration in 166 patients with suspicious breast lesions. *Eur. Radiol. Exp.* **2018**, *2*, 8. [[CrossRef](#)]
130. Lohitvisate, W.; Pumme, N.; Kwankua, A. Mammographic and ultrasonographic features of triple-negative breast cancer compared with non-triple-negative breast cancer. *J. Ultrasound* **2022**, 1–8. [[CrossRef](#)]
131. Cellina, M.; Gibelli, D.; Martinenghi, C.; Giardini, D.; Soresina, M.; Menozzi, A.; Oliva, G.; Carrafiello, G. Non-contrast magnetic resonance lymphography (NCMRL) in cancer-related secondary lymphedema: Acquisition technique and imaging findings. *Radiol. Med.* **2021**, *126*, 1477–1486. [[CrossRef](#)]
132. Fusco, R.; Sansone, M.; Granata, V.; Di Bonito, M.; Avino, F.; Catalano, O.; Botti, G.; Petrillo, A. Use of Quantitative Morphological and Functional Features for Assessment of Axillary Lymph Node in Breast Dynamic Contrast-Enhanced Magnetic Resonance Imaging. *BioMed Res. Int.* **2018**, *2018*, 2610801. [[CrossRef](#)] [[PubMed](#)]
133. Nicosia, L.; Bozzini, A.C.; Palma, S.; Montesano, M.; Signorelli, G.; Pesapane, F.; Latronico, A.; Bagnardi, V.; Frassoni, S.; Sangalli, C.; et al. Contrast-Enhanced Spectral Mammography and tumor size assessment: A valuable tool for appropriate surgical management of breast lesions. *Radiol. Med.* **2022**, *127*, 1228–1234. [[CrossRef](#)] [[PubMed](#)]
134. Romanucci, G.; Mercogliano, S.; Carucci, E.; Cina, A.; Zantedeschi, E.; Caneva, A.; Benassuti, C.; Fornasa, F. Diagnostic accuracy of resection margin in specimen radiography: Digital breast tomosynthesis versus full-field digital mammography. *Radiol. Med.* **2021**, *126*, 768–773. [[CrossRef](#)] [[PubMed](#)]

Disclaimer/Publisher’s Note: The statements, opinions and data contained in all publications are solely those of the individual author(s) and contributor(s) and not of MDPI and/or the editor(s). MDPI and/or the editor(s) disclaim responsibility for any injury to people or property resulting from any ideas, methods, instructions or products referred to in the content.